Digest 2014, December 2014, 1757-1783

Strong Ground Motion Simulations Around Prince Islands Fault†

Aydın MERT*
Yasin FAHJAN**
Ali PINAR***
Lawrence HUTCHINGS****

ABSTRACT

The main objective of this study is to simulate broad-frequency-band strong ground motion waveforms resulting from the rupture of the Prince Island Fault and to provide input accelerograms for linear and non-linear time history analyses for engineering structures. Simulations are performed using Green's Function methodology developed by Hutchings and Wu (1990) [1]. The methodology considers physical based rupture process and takes into account different source parameters to investigate their effects on amplitude and frequency content of simulated waveforms. As a result, the low frequency energy content of the simulated waveforms has significant role in the characteristic of strong ground motion for large earthquake in Marmara region.

Keywords: *Broadband earthquake simulation, green's functions, prince Island fault.*

1. INTRODUCTION

Destructive earthquakes may cause severe damage, particularly within the near source region, which is defined as the area that lies within two fault-lengths from the source. For this reason, determination of strong ground motion for large earthquakes, especially by considering the complex nature of wave propagation at the near source region, is one of the primary objectives of recent engineering seismology studies. The basis of the strong ground motion studies is the prediction of strong ground motion parameters that will originate from potential future earthquakes by defining the faulting mechanisms and the respective affecting parameters of the previous earthquakes.

Realistic characterization of strong ground motions occurring near source regions is highly critical, particularly for civil engineering studies. Recent improvements in calculation techniques in the earthquake-resistant design of engineering structures resulted in the adoption of performance-based design approach and in the widespread utilization of time-history analyses in seismic design of the structures. Classical methods that are used in calculation of seismic loads on structures during earthquakes, such as the 'Equivalent Static

* Boğaziçi Universty, İstanbul, Turkey - mertay@boun.edu.tr
** Gebze Technical University, Kocaeli, Turkey - fahjan@gyte.edu.tr
*** İstanbul University, İstanbul, Turkey - alipinar@istanbul.edu.tr
**** Lawrence Berkeley National Laboratory, Berkeley, USA - ljhutchings@lbl.gov

† Published in Teknik Dergi Vol. 25, No. 3 July 2014, pp: 6775-6804

Earthquake Load Method' and the 'Mode Superposition Method', have been replaced by nonlinear time-history dynamic analysis. Since the latter group of analyses require acquisition of proper seismic records, this has become an important subject of earthquake engineering studies.

There are three sources in the literature, from which strong ground motion acceleration records for dynamic analyses can be obtained: **1)** Actual acceleration records obtained during earthquakes, **2)** Synthetic acceleration records compatible with design acceleration spectrum, and **3)** Simulated acceleration records, which take propagation medium properties into account and use seismologic source models.

Acceleration records obtained from actual earthquakes, are records that have been selected and scaled using certain geological, tectonic, and seismological parameters obtained from the study area. These records not only consist of reliable data regarding the nature and characteristics of the earthquake (e.g., magnitude, duration, phase properties, frequency content), but they also reflect important factors such as the source affecting the seismic wave propagation, properties of the propagation medium and ground conditions [2]. Basic methods and criteria for selection and scaling of actual ground motion records suitable for the earthquake-resistant design of engineering structures is explained in detail in Fahjan (2008) [2].

Synthetic accelerograms, are the artificially generated acceleration time history that are compatible with the response spectrum obtained by seismic risk analysis of a particular region or with the design spectrum specified in the seismic design regulations [3].

Simulated accelerograms, are the acceleration time history obtained through earthquake simulations that model the earthquake source and source region wave propagation using physics-based processes. The simulation procedure, in general, is expressed in terms of elastodynamic representation theory, and it is calculated by taking the integral of the contribution of each point on the fault surface to the ground motion (Green's Function) [4].

The increase in the existing strong ground motion database and the enhanced ease of access to these data as a result of ongoing improvements in the communication technologies enabled the use of real acceleration records in dynamic analyses of structures. However, it becomes difficult to find records that are suitable for design, when other criteria such as ground class, distance between the source and the field, magnitude, and rupture processes are taken into account [5, 2]. Similar difficulties are also encountered in attempting to use the synthetic acceleration records during design. The biggest challenge in the use of artificial acceleration records is to try to obtain a single record suitable for the design spectrum representing the average of numerous recorded ground motions [6, 2]. Another limitation on the use of these records is the unrealistically high amounts of energy released due to an increase in the number of cycles of strong ground motion [2]. During the analysis of nonlinear behaviour of structures, phase information is equally important as the magnitude of the ground motion. This, combined with the scarcity of records for recent and large earthquakes, suggests that both options mentioned above are far from meeting the expectations. Therefore, during dynamic analysis of structures it would be better to use earthquake ground motions that were simulated based on the basis of earthquake physics and with spectral averages that are broadly coincident with the design spectrum [4].

Numerous studies have characterized the entire Marmara Sea as a seismic gap due to the westward migration of destructive earthquakes [7, 8], as indicated by the August 17, 1999 Gölcük (Mw=7.4) and November 12, 1999 Düzce (Mw=7.2) earthquakes and the August 9, 1912 Mürefte-Şarköy (Ms=7.2) earthquake [9]. It is therefore mandatory to accurately determine the bedrock ground motion in a wide-band frequency range to assess the seismic risk potential of the Marmara region and to reliably estimate the future seismic risks. This study aims to provide input data for the linear and non-linear time-space analyses of the structures using a hybrid simulation method and to predict, in a wide-band frequency range, the ground motion waveforms that will be generated by rupturing of the Prince Islands Fault through a potential M_w=7.2 earthquake. In addition, effects of variations in different source parameters on the magnitude and frequency contents of these waveforms are also investigated.

2. EARTHQUAKE GROUND MOTION SIMULATION MODELS

Earthquake simulation models are based on the information on physical properties of the geological environment and the local ground conditions of the area between the earthquake source and the recording station. In addition, the effects of the variations in fault parameters and fault rupture characteristics on strong ground motion records should also be known [10]. Key elements of earthquake simulation models, in general, are the source, propagation direction, and local ground effects [4].

In recent years, numerous studies have been undertaken by seismologists particularly regarding the modelling of earthquake rupture processes in order for accurate prediction of ground motions generated by large earthquakes [1, 11, 12, 13]. There are numerous methods in the literature dealing with earthquake ground motion simulations. These methods can be mainly classified as **Green Function**, **Deterministic**, **Stochastic**, and **Hybrid** methods.

2.1. Green's Function Based Earthquake Simulation Methods

In general terms, the **Green's Function (GF)** can be defined as the reaction of the ground to an instantaneous impulsive point source. This definition is also an expression of the theoretical "Synthetic Green's Function" (SGF) as used in this study. In order to synthetically calculate the GF it is necessary to know the crustal velocity structure of the region between the earthquake source and the recording station. However, it is not possible to determine the heterogeneous nature of the ground with sufficient resolution, especially for the high-frequency or short wavelength components of ground motion. Practically, the problems that stem from this heterogeneity can be best overcome by utilizing the **Empricial Green's Functions (EGF)**, which includes the effects of crustal velocity structure [14]. The EGF method, which was first proposed by Hartzell (1978) [5] and Wu (1978) [16], is based on the principle that earthquake rupture and resulting ground motion can be modeled based on the elastodynamic represention theory and using the ground motion information recorded from small earthquakes. This method was later modified, improved, and utilized by some other researchers in their studies such as Hadley and Helmberger (1980) [8], Irikura (1983) [13], Hutchings and Wu (1990) [1], and Hutchings

(1991) [10]. The basis to this this method is to utilize the observed small earthquakes originating from the rupture area of the simulated large earthquake to count on the actual propagation medium and local effects, and thereby determine, with great accuracy, the asperity fields in the source and the heterogeneity [15]. A schematic presentation of earthquake simulations developed using GF is provided in Figure 1.

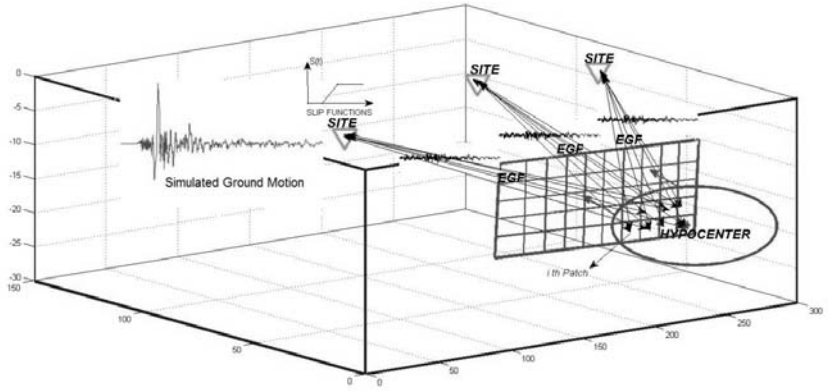

Figure 1. Schematic illustration of Green's Function simulations.

2.2. Deterministic Earthquake Simulation Models

Deterministic earthquake simulations, utilizing kinematic source models, require the knowledge of fault slip distribution. In principle, deterministic methods combine SGF with source function to generate surface ground motion during an earthquake [4]. In order to determine the ground motion at any point by this method, the earthquake source geometry, slip functions for the entire source, and the GF should be defined and the source needs to be divided into a finite number of discrete elements [14]. Finite difference, finite element, and discrete wave number methods are the most commonly used approaches used in the literature in generating deterministic strong ground motion simulations. Aki (1968) [17] and Bouchon and Aki (1977) [18] are two of most significant studies in this field that developed and utilized this model.

2.3. Stochastic Earthquake Simulation Models

Stochastic method is one of the most widely utilized strong ground motion simulation models, and it is based on the assumption that the high frequency components of earthquake motion can be represented by an omega-squared (ω^2) average spectrum based band-limited Gaussian noise [12]. Erdik et al. (2003) [4] indicated that the Fourier magnitude spectrum model used in stochastic earthquake simulations is an S-wave ground motion spectrum based on the far-field model of Brune (1970) [19]. The Fourier magnitude spectra of Brune (1970) [19] are satisfied by the main parameters of high frequency ground motion for earthquakes within a wide magnitude range [20]. Basic steps of the earthquake

simulations using the stochastic method are shown in Figure 2. In general, two different source models, point source and finite source, are used in stochastic simulation techniques [2]. The point source model, in which the source is localized into a single point, is based on the assumption that the obtained waveform simulation model involves both deterministic and random processes. The point source model yields highly accurate results when the distance between the source and the receiver is significantly larger than the dimensions of the source itself [21, 22]. Beresnev and Atkinson (1997) [23] developed a method for finite-

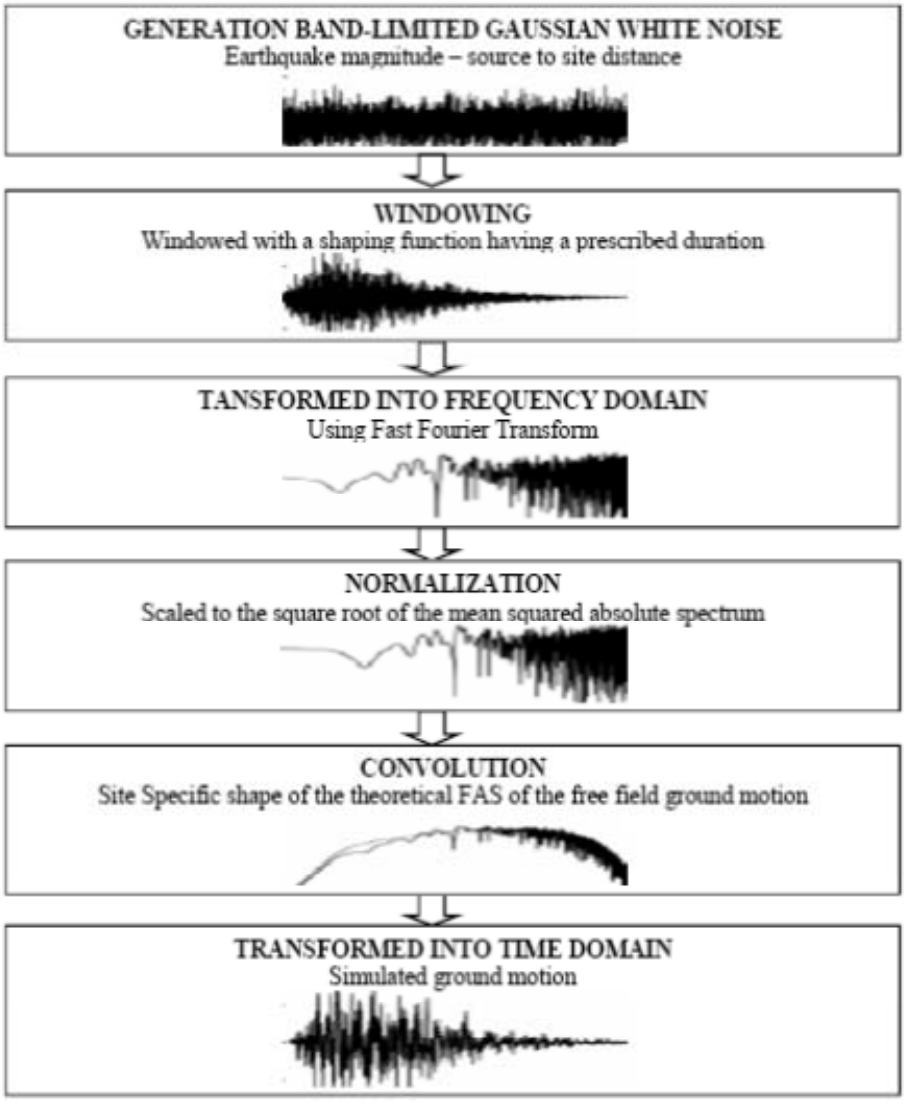

Figure 2. Basic step in Stochastic earthquake simulations.

fault strong ground motion simulation [4] by modeling the fault rupture plane as a subfault matrix and by considering propagation originating from each subfault as a subfault point source with ω^2-model spectrum (in conjunction with the principles of [12]). The finite source model solved an important problem in stochastic earthquake simulation techniques, since it involves finite-fault rupture effects (e.g., source geometry, uncertainty in rupture parameters, nonhomogeneity, etc.), which cannot be modeled by stochastic point source models.

2.4. Hybrid Broadband Earthquake Simulation Methods

During generation of broadband strong ground motion simulations by the hybrid approach, first the ground motion components from different frequency bands of the spectrum are determined individually, and then these data are combined together. Recent seismologic developments make the mathematical solution of the SGFs possible for the large wavelength (or low frequency) components, for which the geological heterogeneities can be modeled. High frequency components of ground motion, on the other hand, cannot be mathematically solved due to uncertainties related to the earthquake source and the geological heterogeneities. As a result, these components should be calculated either by stochastic simulation techniques of high-frequency components of the strong ground motion or by utilizing an EGF-based method that uses small earthquake records as a GF. Both low and high frequency band components of earthquake ground motion are determined through different methods, and these are later combined via specific filtering functions to obtain ground motion simulations within a wide frequency range. Designing of the filtering functions that will be used during combination processes is a particularly important subject as energies obtained from different parts of the spectrum need to be combined properly.

3. BROADBAND EARTHQUAKE SIMULATIONS OF THE PRINCE ISLANDS FAULT

A considerable amount of studies exist in the literature in which bedrock ground motion is calculated by hybrid broadband simulation techniques, in order to accurately assess the seismic risk and potential future seismic risk evaluation of the Marmara region, particularly following the 1999 earthquakes [24, 25, 26, 27, 28, 29]. These studies presented important results in terms of complexity of ground motions that may be produced during a large earthquake. Tanırcan (2012) [24] obtained a simulation of strong ground motions that can be recorded at 82 acceleration stations in İstanbul during a potential M_w=7.2 earthquake along the Prince Islands Fault. He determined acceleration values of up to 8 m/s^2 in the Asian side and velocity values of up to 1.6 m/s by using finite difference method for the low frequency ground motion simulations, and by hybrid simulation with stochastic techniques for the high frequency ground motion simulations. Erdik et al. (2001) [25] calculated design-based strong ground motion waveforms for critical engineering structures that are located in the near-fault regions. In this study, they utilized a hybrid method in which they combined the low frequency ground motion components determined by deterministic methods with the high frequency ground motion components determined by stochastic methods, and generated broadband ground motion waveforms. Similarly, Pulido

et al. (2004) [26] calculated the low frequency ground motion components through a deterministic algorithm, and the high frequency components by a semi-stochastic method, and examined the variations in some important ground motion parameters for the engineering structures such as the absolute amplitude, frequency content, and duration of the earthquake, for a potential large earthquake in the Marmara region. Mathilde et al. (2007) [27] used a hybrid model similar to that of [26] and demonstrated the potential effects of source and attenuation parameters on strong ground motion waveforms that may form during a large earthquake in the Marmara region. Ansal et al. (2008) [28] obtained strong ground motion simulations for İstanbul by using a stochastic-deterministic hybrid approach, and attempted to predict the potential damage and loss that will occur following a large earthquake. Using a hybrid model, Mert (2011) [29] determined the strong ground motion waveforms, which may form during a large earthquake in the Marmara Sea, in a wide frequency range, thereby demonstrating the dependency of the ground motion to source and rupture parameters, by implementing different earthquake scenarios. Prior to the current study, no other work has utilized an EGF-based simulation technique along the fault segments traversing the Marmara Sea. This is most likely due to a lack of data relating to the insufficient number of good quality earthquake stations. Nevertheless, different organizations have installed a number of broadband earthquake stations have been installed in the region, particularly following the 1999 earthquakes, allowing new geophysical and geological studies [30, 31, 32, 33, 34, 35, 36, 37, 38, 39, 40, 41] within or in the vicinity of the Marmara Sea.

In this study, hybrid simulation algorithms are utilized to simulate broadband strong ground motion waveforms resulted from a possible earthquake of moment magnitude Mw=7.2 at Prince Islands fault. The seismic criteria of the Prince Islands fault are selected to be compatible with the current studies in the literature. Maximum possible earthquake at Prince Islands will generated with fault rupture length of 35-40 km [42, 24] and the seismic moment-earthquake magnitude empirical relationship [43] and the empirical relationship between fault size and earthquake magnitude [44] are chosen accordingly.

Empirical and synthetic Green functions are used for the simulations of wave propagation for high and low frequency bands. The physical based fault ruptures and wave propagation methodology proposed by Hutchings and Wu (1990) [1] is used to simulate the strong ground motion waveforms. In order to consider the variation in the fault rupture mechanism, 100 different scenario are generated.

The parameters related to fault geometrical properties and rupture mechanism and earthquake source (hypocenter, depth, rupture velocity, etc.) are considered. The variation and limits of fault parameters are based on different studies in the literature. The selected earthquake scenarios are based on studies related to tectonic structure of the Marmara region [30, 31, 32, 33, 34, 35], earthquake source parameters [36, 37], seismic moment-earthquake magnitude [43], empirical relationships of fault size - earthquake magnitude [44] and other related studies [42, 24].

For each earthquake scenario, the Green functions recorded from small earthquake at Prince Islands fault are used for the simulation of high frequency of the strong ground motion waveforms. The low frequency part of the waveforms are simulated using synthetic Green functions resulted from finite difference model developed by Shawn Larsen (Lawrance Livermore National Laboratory, LLNL) (1995) [45]. The model simulates the propagation

of seismic waves resulted from a seismic source in three dimensional elastic medium that represent the geological characteristics of the region. Finally, the low frequency and high frequency strong ground motion waveforms are merged to produce broadband waveforms for the range (0.1 Hz–20 Hz). Special filtering algorithms are used for merging process. As it is shown in Figure 3; four different softwares are used to produce the broadband simulated waveforms, NETMOMENT, EMPSYN, E3D and HAZARD.

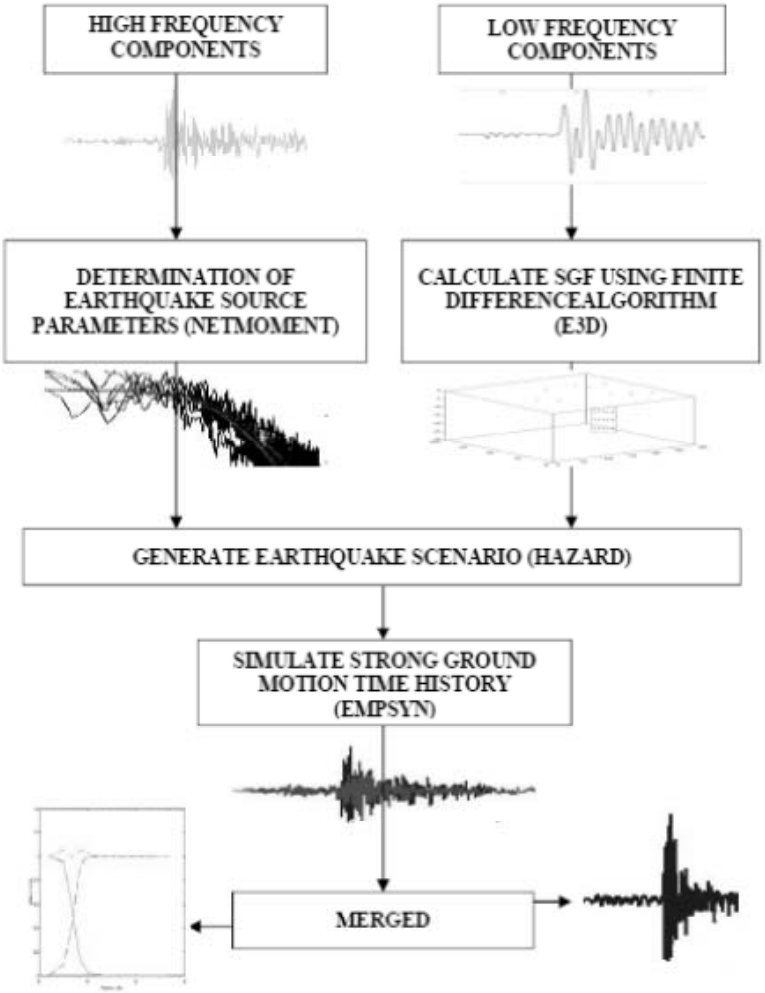

Figure 3. Basic step of simulation algorithm that was used to generate strong ground motion waveform. High frequency components of waveforms simulated using by EGF and low frequency components of waveforms simulated using by SGF. High frequency and low frequency simulated waveforms merged to obtain broadband strong ground motion.

3.1. Broadband Earthquake Waveforms Simulations

3.1.1. Synthetic Green Functions for Low Frequency Simulations

In order to produce broadband simulation for different earthquake scenarios of Prince Islands fault, the low frequency synthetic Green function needed to be generated. For this purpose, a three dimensional volume is introduced with 300 km length in East-West direction and 200 km width in North-South direction, with a starting point 40.0 N 26.50 E (Figure 4). The dimensions are selected to comprise all stations for the simulations. The Prince Islands Faults are placed at the coordinates 40.887 N 28.866 E and 40.732 N, 29.244 E with fault width 15 km and fault depth 10 km from the surface. The shear velocity model proposed by Karabulut et al, (2003) [46] are used for the simulation. The proposed stations' locations for the simulations are placed at the surface of the volume taken into account their spatial coordinates.

The earthquake sources are placed laterally on the fault every 7 km and at three depths (12.5 km- 17.5 km- 22.5 km), therefore 15 earthquake sources are used to produce the synthetic Green functions. The seismic moment of the earthquake source is considered to be M0=1e+21 dyn.cm and corner frequency 10 Hz. The fault mechanism of the earthquake sources are chosen to be compatible with the Prince Islands fault mechanism with strike 118° dip 90° and rake -180°. The volume is discritized with 0.5 km grids and time step of 0.01 is chosen for output synthetic seismograms. In Figure 5, the generated synthetic seismograms of station ADV is shown.

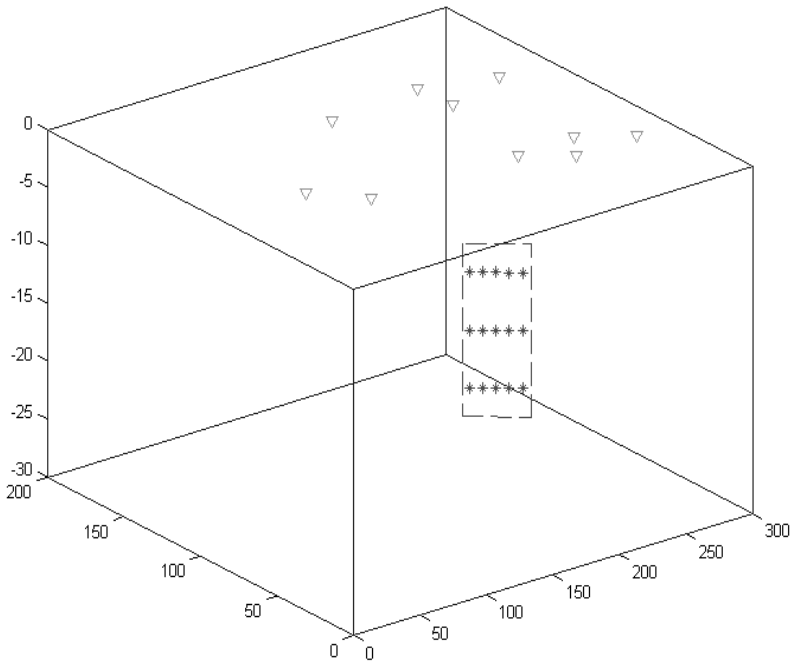

Figure 4. Finite difference model for synthetic seismograms of Prince Islands Fault (Red stars is earthquake source points, Green triangles are station locations)

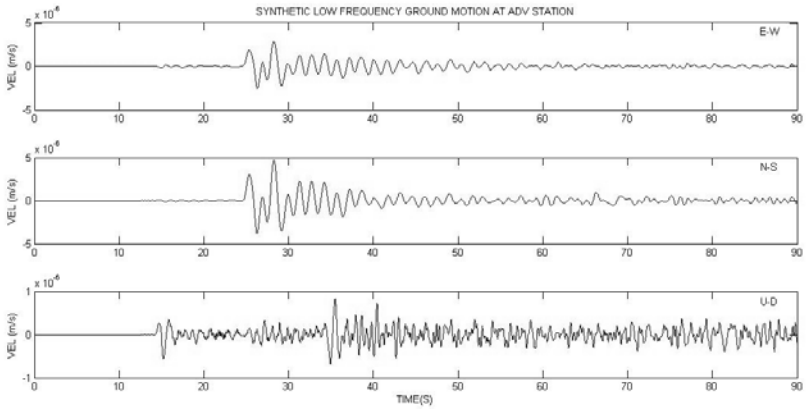

Figure 5. Simulated synthetic seismograms for ADV Station.

3.1.2. Empirical Green Functions for High Frequency Simulations

To generate the high frequency part of the broadband earthquake simulation, the real recorded Green functions are used. The Green functions of small earthquakes (Mw≈3.5) in Marmara Sea at the vicinity of Prince Islands fault are recorded at the broadband stations around Marmara Sea.

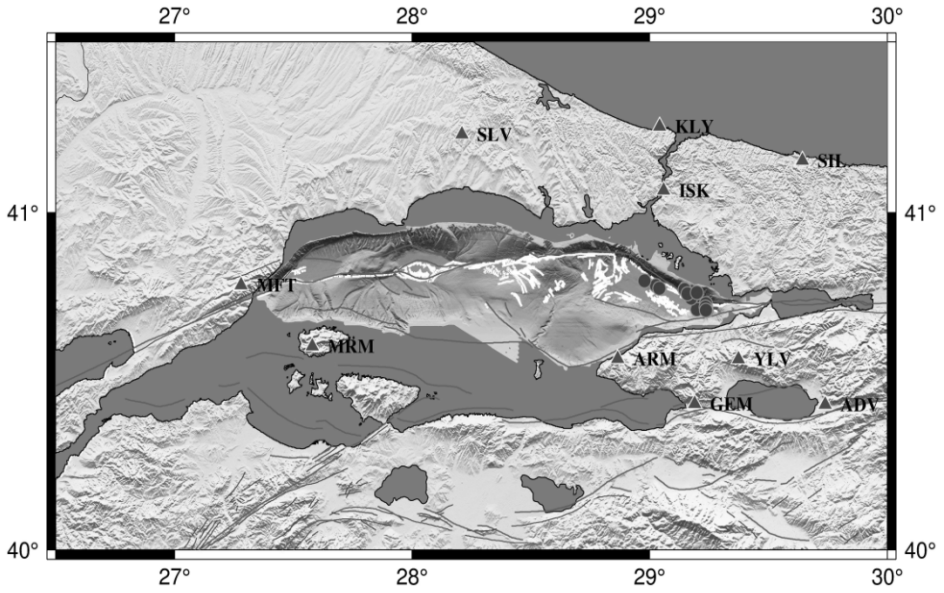

Figure 6. Small Earthquakes used as Green's functions at Prince Island Fault and recording stations.

Table 1. Earthquake stations recorded Green's functions at Prince Islands Fault.

NO	Station Code	Latitude (N) Degree	Longitude (E) Degree	Seismometer Type
1	ADV	40.4332	29.7383	CMG-3TD
2	ARM	40.5683	28.8660	CMG-3ESPD
3	GEM	40.4350	29.1890	CMG-3TD
4	ISK	41.0657	29.0592	CMG-3TD
5	KLY	41.2530	29.0420	CMG-3TD
6	MFT	40.7867	27.2812	CMG-40T
7	MRM	40.6058	27.5837	CMG-3TD
8	SIL	41.1530	29.6430	CMG-3ESPD
9	SLV	41.2300	28.2100	CMG-3ESPD
10	YLV	40.5667	29.3728	CMG-40T

Table 2. Green's functions and source parameters at Prince Islands Fault

NO	DATE (dd/mm/y)	Hour (Local)	Latitude (N) Degree	Longitude (E) Degree	Depth (Km)	M_w	MOMENT (Dyne-cm)	f_c (Hz)
1	290904	15:42	40.785	29.027	13.4	3.9	76.4 e+20	12.3
2	290904	15:51	40.777	29.041	10.77	2.9	2.84 e+20	8.3
3	070905	13:22	40.732	29.237	7.6	3.4	13.1 e+20	10.2
4	080905	00:22	40.715	29.199	12.1	3.1	4.22 e+20	4.5
5	080905	03:39	40.711	29.241	5.4	3.2	6.01 e+20	8.6
6	080905	07:12	40.722	29.235	9.8	3.2	8.44 e+20	6.1
7	031105	05:06	40.712	29.237	14.7	3.2	8.4 e+20	11.0
8	221008	01:00	40.748	29.174	9.4	3.8	63.6 e+20	4.2
9	160406	20:54	40.773	29.147	24.6	3.0	3.84 e+20	10.2
10	120906	18:18	40.799	28.978	10.4	3.0	3.72 e+20	11.7
11	280507	22:47	40.761	29.159	7.9	2.7	1.31 e+20	12.1
12	030208	12:57	40.764	29.198	5.3	2.7	1.45 e+20	14.3

The stations used for the simulations are listed in Table 1 and shown in Figure 6. The green functions for small earthquakes recorded at the listed stations are shown in Figure 6, and the calculated source parameters are given in Table 2. The main advantage of using real earthquake records s Green's functions along the fault surface is that these records include all the geological information across the propagation path. In addition, the recorded green functions also contain the information about the linear response of the upper soil.

The distribution of the small earthquake sources at the fault surface to represent the propagated energy from all the regions across the fault surface practically is not possible. During the simulations, interpolations of the recorded Green's functions for all the regions

across the fault surface are performed. One another important point to use representation relations, selected earthquakes used as EGF must provide effectively impulsive point source conditions or in other words their moment must be below a threshold (about 1.5*1014 Nm) [1], [47]. If moment value of the earthquake used as EGF larger than threshold than deconvolve out source effect from the spectrum to provide effectively impulsive point source [48]. This procedure was applied some of the EGF used in this study.

3.1.3. Computation of source parameters of Empirical Green's Functions.

The source parameters, seismic moment (Mo), corner frequency fc) and damping parameter (t*) are calculated directly from the horizontal components of S waves.

During the analyses, horizontal components of the record related to a specified station are converted to radial and transverse components with respect to seismic source, and then the first 12 seconds of S waves are used to compute the source displacement spectra. For each earthquake, the source parameters Mo, fc and t* are computed using simultaneous inverse solution techniques as it is explained in Hutchings (2001) [47]. In order to eliminate the effects of damping at certain frequencies between the stations along the path they were recorded with respect to the earthquake sources, the available studies in literature regarding Marmara region were reviewed. The frequency dependent quality factor of the shear waves relationship, $Q(f) = 180\ f^{0.45}$, proposed by Akinci et al. (2006) [49] are utilized. The wave propagation geometrical scattering effects (R^{α}) on displacement spectra are removed using the factor α=0.5 for distances greater than 100 km and α=1.0 for distances less than 100 km. 1D shear velocity model proposed by Karabulut vd. (2003) [46] is used in the analysis. The free surface correction coefficient (S) is computed form the shear velocity model; together with the densities, the P waves velocity (V_p) is calculated [50].

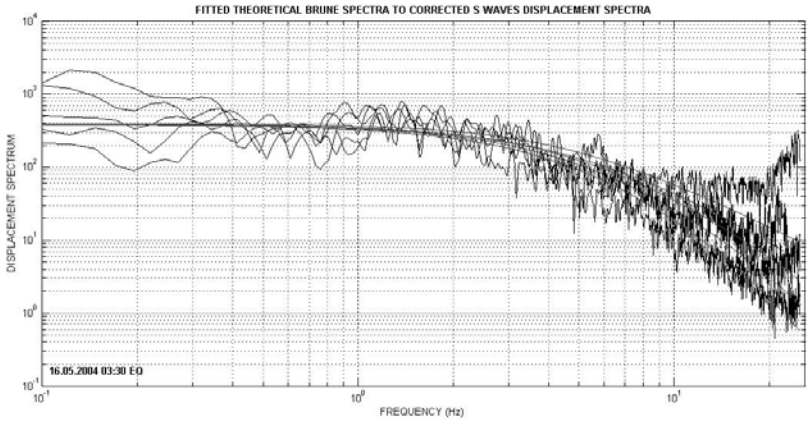

Figure 7. Fitted theoretical Brune Spectra to corrected S waves displacement spectra of the recorded earthquake (Red lines represent Brune spectra, Black lines represent observed S waves displacement spectrum. The radial and transverse components of S waves of the stations ISK, KLY, MRM, SLV, YLV are used)

The focal mechanism radiation correction factor (F) of 0.47 and 0.52 [51] was used for SV and SH arrivals, respectively. The local soil effects on the displacement spectra could not be removed since the soil response functions are not known. Therefore, local site effect is considered to be the reason for scattering of the results.

During the analysis algorithm conducts a signal to noise ratio of the data before performing to inversion, and only frequency ranges of the recorded spectra above a selected Signal to Noise Ratio (SNR) are used in fitting the Brune model to calculate source parameters of selected earthquakes. We used a SNR of 10. Figure 7 shows an example of how we fit spectra simultaneously for source and individual station. In the figure we used 16.05.2004 03:30 earthquake time history recorded by Marmara (MRM) station and fitted Brune spectrum and recorded spectrum in the frequency range between 0.15 to 25 Hz. We used a nonlinear least squares best fit of displacement spectra of the S wave energy of the recorded seismograms fit to Brune (1970) [19] displacement spectral shape with a site specific attenuation operator to solve our free parameters (Figure 7).

3.1.4. Generation of earthquake scenarios of Prince Island fault

To generate different earthquake scenarios for Prince Islands fault, fault geometry, location of the hypocenter, size and number of asperities, rupture velocity, strike and rake vectors together with measured or theoretically determined parameters such as stress drop are changed randomly in physically possible ranges. Then, synthetic and empirical Green's functions are used separately for the simulations of low and high frequency bands for all scenarios.

The basic hypotheses premise of the methodology is that if a particular fault segment is identified as capable of having an earthquake of particular moment, and if sufficient variations of rupture parameters are sampled, then the suite of synthesized seismograms would encompass all possible seismograms, in an engineering sense, and they can be used earthquake resistant design of structures [52].

The parameters and variations intervals used in the scenarios are described below;

Moment; seismic moment values for Princes Islands fault are considered to be in the range M_0=0.5e+27 Dyne-cm to M_0=1e+27 Dyne-cm

Fault rupture geometry; The shape of the fault is considered to be rectangular with 35 km length and 15 km width and 10 km depth from the top boundary of the fault to the surface.

Fault strike, dip and rake; Considering current tectonic and seismological studies in the literature regarding Prince islands fault is modeled as strike-slip with the following parameters ranges: Strike 110 ° / 116 °, dip: 70 ° / 90 °, rake: -160 ° / 180 °.

Hypocenter, randomly changed on the fault, therefore each scenario has different depth and coordinates.

Rupture velocity is randomly selected to be from 0.8 to 1.2 times the shear wave velocity.

Healing velocity is the velocity for the stress pulse that terminates slip. The healing phase is initiated after rupture arrives at any fault edge. The healing velocity is randomly selected

to be between 0.8 and 1.20times the rupture velocity, which is between the Rayleigh and shear wave velocities.

Rise time is equal to the time it takes, after the initiation of rupture, for the first healing phase to arrive.

Rupture roughness is modeled by delaying an element's rupture time so that it finishes slip (rise time) at the same time as neighboring elements. The delay is randomly chosen to be 33 % of the original rise time of the element. Areas of roughness have ("rough" elements) have corresponding high stress drop.

Stress drop is a dependent variable derived from the Kostrov slip function [53] and allowed to vary according to three effects modeled in the rupture: asperities and rough rupture are allowed to have a different stress drop from surrounding portions of the fault rupture; stress drop is constrained to diminish near the surface of the earth. The near surface stress is the minimum calculated from confining pressure and stress drop from the rupture model.

3.1.5. Merging Earthquake Simulations at Low- and High-frequency bands

Several methods have been developed on the integration of low and high frequency seismograms used for estimation of the broadband (0-20 Hz) hybrid waveforms in earthquake engineering applications ([54] Irikura and Kamae, 1994; [55] Beresnev and Atkinson, 1997; [56] Kamae et al, 1998; [57] Hartzell et al., 1999; [58] Pitarka et al., 2000; [59] Pulido and Kubo, 2004; [60] Graves and Pitarka, 2004; [61] Mena et al.., 2006; [62] Pulida and Matsuoka, 2006; [63] Liu et al., 2006; [64] Rodgers et al., 2008, see [65] Mai et al., 2010, pp.2128 for more references).

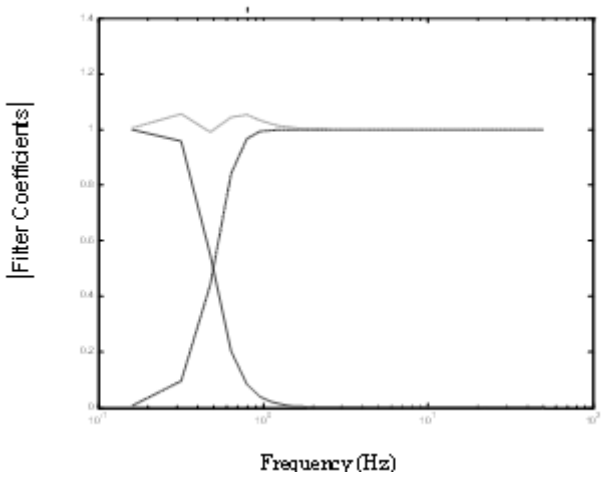

Figure 8. The filter functions used to obtain the broadband earthquake simulations.

In this study, we obtained earthquake simulations at wide band frequencies (0.1-20.0 Hz) for each seismic station, using in-house merging algorithms in MATLAB environment, by merging the low and high frequency band simulations estimated for different earthquake scenario. The GF synthetics at low frequencies (0.1-2.0 Hz) calculated using finite difference algorithms yield reliable results by taking into account the grid size (0.5 km) and the structural features of the seismic seismic velocity model.

The sampling rate of the earthquake records used as EGF in high frequency band is 0.02 s thus providing high frequency components up to 25 Hz Nyquist frequency in the spectra. However, because of the noise level characteristic of the smaller size earthquakes the preferred frequency band was selected as 0.5-20 Hz and in the merging algorithm we used the 0.5 Hz frequency as the pivot frequency.

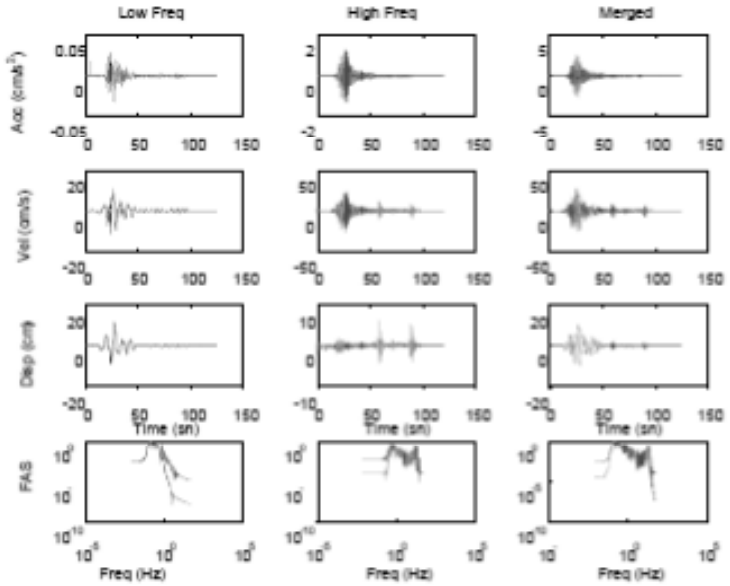

Figure 9. Integration of the simulation results obtained for low and high frequency bands at ARM station (blue color is the original seismogram, while the red color is the filtered seismogram).

In broadband earthquake simulation spectra, for the frequencies below 0.5 Hz the simulations are obtained by low pass filtering the SGF seismograms, while for the frequency higher than 0.5 Hz the simulations are obtained using high-pass filtering of the EGF functions. An optimization process was applied to choose the appropriate filtering coefficients and the sum of the coefficients of the merging filter in frequency domain was set to be as close as possible to one. This process, in turn, prevented large amplitudes to appear around the corner frequency of the integrated broadband ground motion simulations. The filter functions used in this study are portrayed in Figure 8.

Figure 9 illustrates the merging results of the low and high frequency simulations at ARM station for one of the 100 scenarios using the filter coefficients described above. The blue color seismograms in the first column of the figure are the low frequency SGF simulations while the red colors seismograms are the filtered simulations derived using the filter function shown in Figure 8. The second column shows the high frequency original and filtered simulations, and the third column indicates the original and the filtered seismograms attained from the low and high frequency components of the simulations.

The average acceleration, velocity and displacement seismograms estimated for the two horizontal components are derived from the average and the standard deviation of the 100 broadband earthquake simulations acquired for each seismic station and are given separately in the figures from 10 to 19.

4. RESULTS AND DISCUSSIONS

The studies using different simulation techniques carried out in Marmara region as well as in the other tectonically active regions of the World revealed the limitations and the uncertainties in the modeling of the ground motions likely to be generated by future large earthquakes, even using highly reliable simulation techniques [27].

One of these limitations emerge from the uncertainties in the attenuation parameter of the medium and the source parameters of the earthquakes [27]. The most important advantage of the simulation method of this study is that the attenuation features represent the physical properties of the medium because they are estimated directly from the smaller size earthquakes (EGF function) that take place on the fault to be modeled.

It is proposed that an optimum solution for solving the uncertainty problem of the source parameters is to establish the best and the worse scenario and then determine the limits of the different source parameters for those scenarios [27]. Thus, it is possible to estimate the maximum and the minimum amplitudes of the ground motions to be generated within certain error limits. By virtue of this fact, 100 different scenarios were generated by changing each source parameter values within the limits that are physically likely to be realized.

By applying a physics based rupture process technique, we have estimated the ground motion waveforms to be generated by a Mw=7.2 size earthquake rupturing the Prince' Islands fault segment of the North Anatolian fault crossing the Marmara Sea. We estimated the broadband (0.1-20.0 Hz) synthetic seismograms and compared their spectral contents at 10 seismic stations around Marmara sea and investigated how the variation in the source parameters affect the amplitude and frequency content of the ground motions (Figures 10-19). For this purpose, we used the EGF functions retrieved from the records of the smaller events and the SGF functions estimated using a finite difference method.

Thus, the earthquake source features were determined and when necessary the source effect removed EGFs and the SGFs estimated assuming point sources were scaled to the seismic moment of the expected large earthquake through the representative theorem [66]. The largest problem we faced in determining the source parameters of the smaller earthquakes to be used as an EGF function was the site effects masking the corner frequency of the smaller earthquakes resulting in wrong estimation of the source parameters. For this reason,

we haven't included the data of the stations facing such considerable site effects in the analysis; also, we used the frequency bands where the signal-to-noise ratio was larger than 10 to get rid of the mentioned problems. Another limitation of the earthquakes to be used as EGF was the distance between the events and also their distances to the related fault plane. In this study, we successfully used the EGFs within 8-10 km distance to the fault.

The properties of the earthquake ground motions recorded at the surface depends on faulting geometry, the maximum slip amount, the slip distribution on the fault plane and the rupture pattern. Because of the properties of the quassy-dynamic model we use a change in one of the source parameters results in variations at the other parameters. For example, a change in the rupture velocity results in different rise time and slip distribution. Similarly, a modification in the hypocenter parameter results in variations in rise time and the slip distribution model. In our scenarios we modified several parameters to check how the amplitude and the frequency content of the seismograms vary. When we elaborate the scenarios we observe that the hypocenter location, the rupture velocity and the rise time are the most important source parameters that affect the modeled ground motions. Especially, the stress drop parameter affects the high frequency content of the ground motions. Similar results were previously reported in the literature [24, 27].

How the alterations in different parameter affect the ground motions can be inspected from the spectra obtained for each seismic station (Figures 10-19). One may notice the distinct differences in the energy content of the earthquake simulations attained for different scenarios at the same station. For example, we observe as large as 2-3 times difference in the average energy content and its standard deviation estimated for 100 earthquake scenarios at ADV station (Figure 10). Similar features are achieved at the spectra of the rest of the nine stations for which we get simulations. Thus, it is obvious that the source parameters definitely modify the amplitude and frequency of the waveforms.

Another distinguished aspect of our results is the dominant low frequencies in the simulated waveforms. This finding gives clue on the characteristics of the ground motions to be generated by the large earthquakes (M>7) expected in Marmara region. It is obvious that earthquakes of this size, considering the fault rupture length and the rupture duration should yield rather small corner frequency. Therefore, it would not be a surprise if significant seismic energy release occurs at the lower frequencies. The amplitude spectra of the simulations are kind of proof of the expectations. As such, it is an important issue to be considered during the design of the high-rise buildings, viaduct and bridges because of their large natural periods. Almost all the stations used in the simulations are located at the area described as near-source region. The spectra of the waveforms recorded at the near-source region are expected to possess low-frequency seismic energy due to directivity effect. It is important to state that, the reliability and the success of the method in modeling the earthquake ground motions is proved by the fit of the simulations to such observations.

The average PGA values of the broadband earthquake simulations at the seismic station retrieved from the 100 earthquake scenarios are compared with the GMPE estimations [67, 68, 69] which shows that almost all the values fall within ±1 standard deviation (Table 3). The stations that do not apply for these results are MFT, SLV and YLV which yield PGA values exceeding the ±1 standard deviation range. The difference in the MFT station is so small that one may omit such conclusion. Considering the larger simulation values at the other two stations compared to the estimations from the ground motion prediction equations

and taking into account the location of those stations suggest that a directivity effect might be a causative for the observed difference. Moreover, it is a well-known fact that the GMPE equations do not reflect very well the wave propagation effects at near-source regions [70]. Also, there are several such examples in the literature showing scattering in the results that can't be properly explained. Here, we just compare the average value of the simulated earthquake with the GMPE estimations; whereas, our results exhibits scattering similar to the GPME estimations where we obtain values well above and below the average of the simulated earthquake.

Applying a simulation technique covering several earthquake rupture scenarios on the Prince's island fault we obtained results showing the amplitude and frequency content of the ground motions at several residential area around Marmara Sea. As such, our study is a contribution to the existing literature on the subject and we believe that a comparison of our results with the ones obtained at other tectonically active regions in the World using different simulation techniques would be a benefit to other researchers.

Next, we are planning further studies related with the subject that will be conducted using similar scenarios but using different simulation techniques; then, the results will be compared with the ones we get in this study so as to investigate the ground motion variations. Here, we show that the most effective parameters on the estimation of the ground motions are the source parameters that should be further elaborated in greater details. Considering the multiple fault segment tectonics of Marmara region, we think that our contribution will fill an important gap in the literature dealing with seismic hazard studies based on simulation algorithms.

Table 3. Comparison of the PGA values from the simulations with those obtained from the GMPE estimations at different R_{JB} distances. AS08: Abrahamsan & Silva 2008 [67]; BA08: Boore & Atkinson 2008 [68]; CB08: Campbell & Bozorgnia 2008 [69].

İST	**R_{JB}**	**AS08 (PGA-mg)**			**BA08 (PGA-mg)**			**CB08 (PGA-mg)**			**SIMUL**
		Med	**+1.σ**	**-1.σ**	**Med**	**+1.σ**	**-1.σ**	**Med**	**+1.σ**	**-1.σ**	**(PGA-mg)**
ADV	62.85	51,56	89,95	29,55	72,02	126,6	40.97	53,40	90,27	31,90	80
ARM	15.59	174,6	303,9	100,3	198,2	348,3	112,8	152,9	258,1	90,53	120
GEM	39.41	73,8	128,7	42,32	110,4	194,0	62,8	78,49	132,7	46,45	80
ISK	22.26	125,9	219,4	72,28	162,9	286,4	92,70	121,0	204,4	71,64	125
KLY	41.47	71,04	123,9	40,73	106,0	186,2	60,28	75,30	127,3	44,57	110
MFT	131.0	25,53	44,56	14,62	25,66	45,09	14,60	28,43	48,08	16,81	12
MRM	106.4	32,79	57,22	18,79	36,51	64,17	20,77	34,04	57,56	20,13	28
SIL	42.06	70,29	122,6	40,31	104,7	184,1	59,59	74,48	125,9	44,07	40
SLV	75.49	44,58	77,79	25,55	58,54	102,9	33,30	45,72	77,30	27,04	135
YLV	33.88	82,42	143,7	47,27	123,8	217,5	70,41	88,48	149,5	52,36	270

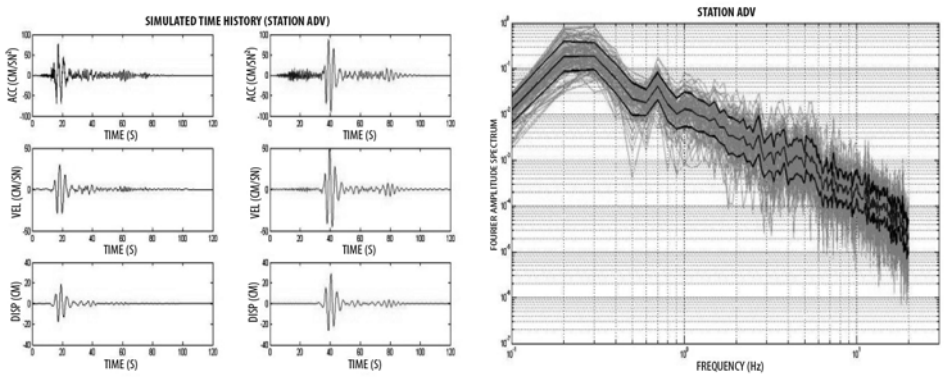

Figure 10. Broadband earthquake simulations obtained for 100 different scenarios at ADV station. Lightblue: the 100 different FGS estimations; red: the average FGS for the simulated earthquake; blue: standard deviation (right panel). Waveforms of the two horizontal components estimated for the average earthquake (left panel).

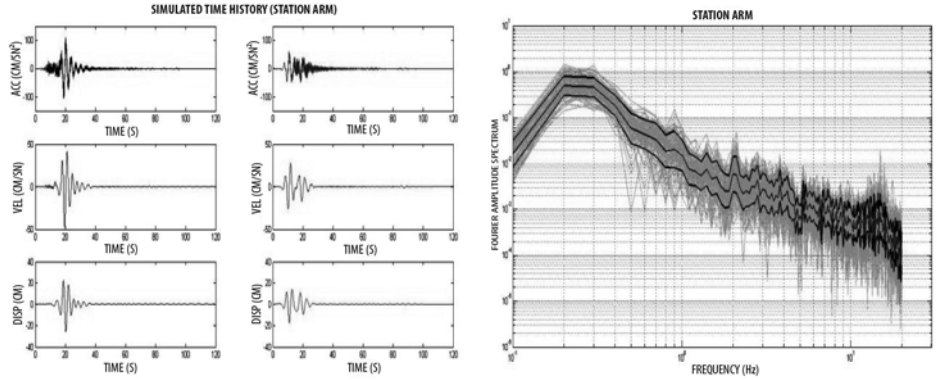

Figure 11. Broadband earthquake simulations obtained for 100 different scenarios at ARM station (see Figure 10 for more explanations).

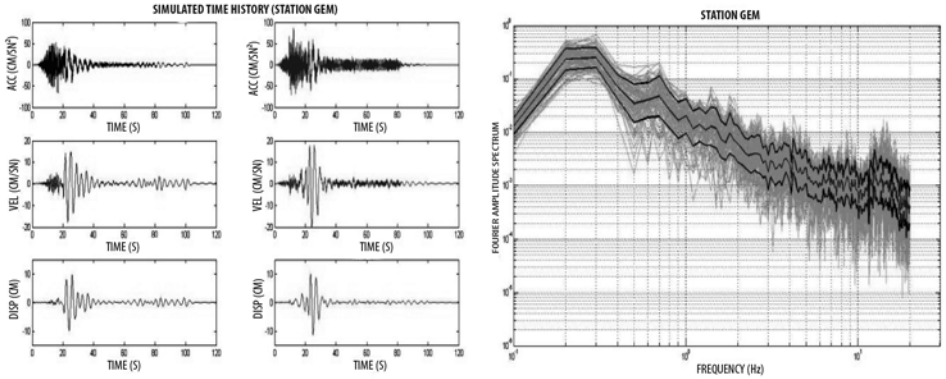

Figure 12. Broadband earthquake simulations obtained for 100 different scenarios at GEM station (see Figure 10 for more explanations).

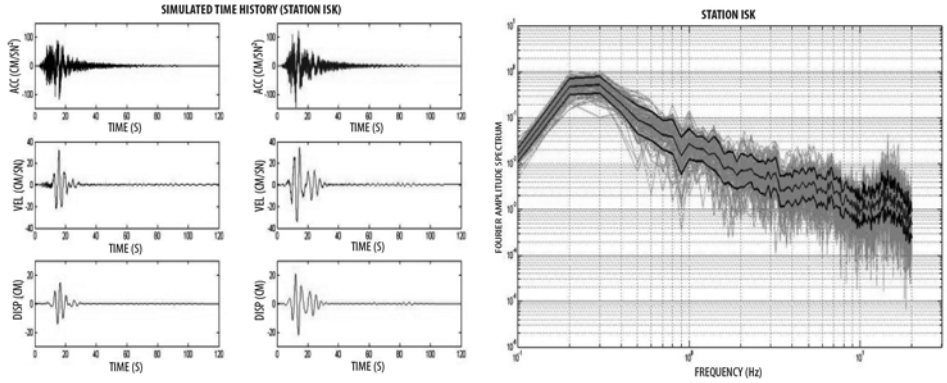

Figure 13. Broadband earthquake simulations obtained for 100 different scenarios at ARM station (see Figure 10 for more explanations).

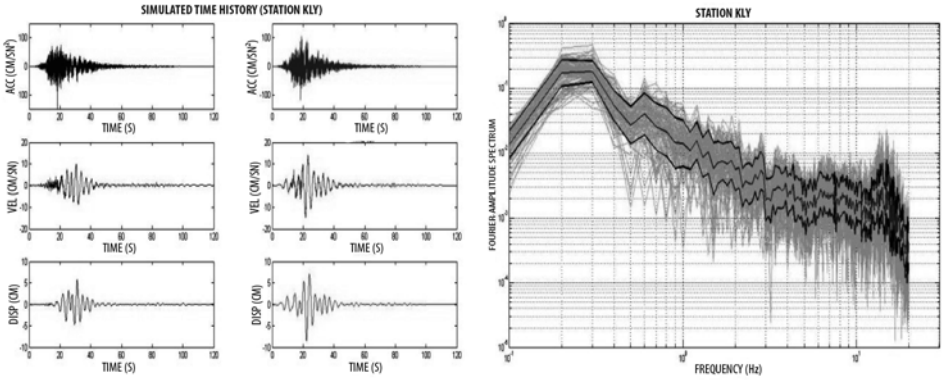

Figure 14. Broadband earthquake simulations obtained for 100 different scenarios at KLY station (see Figure 10 for more explanations).

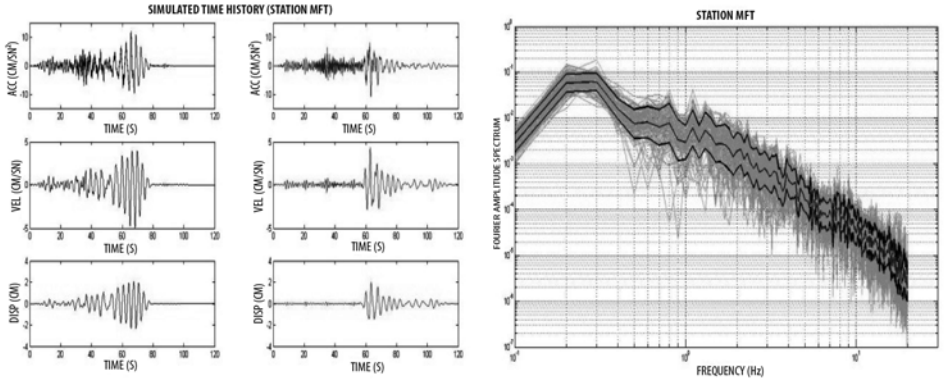

Figure 15. Broadband earthquake simulations obtained for 100 different scenarios at MFT station (see Figure 10 for more explanations).

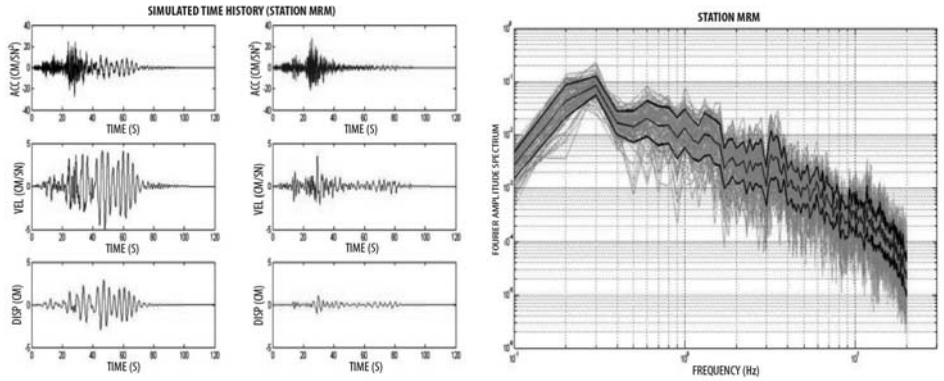

Figure 16. Broadband earthquake simulations obtained for 100 different scenarios at MRM station (see Figure 10 for more explanations).

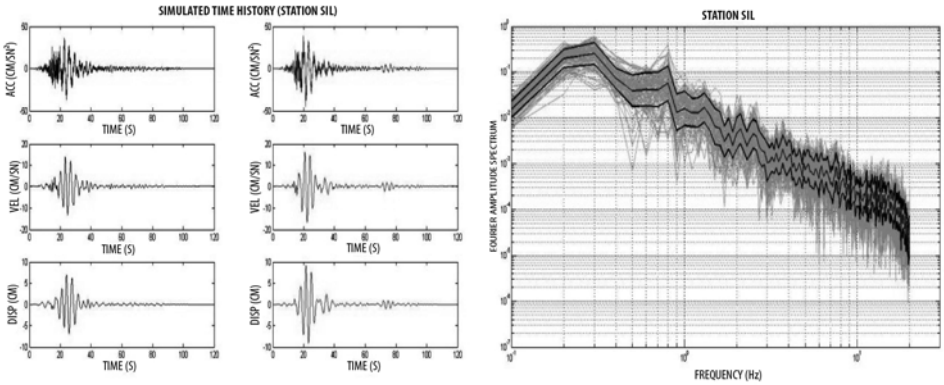

Figure 17. Broadband earthquake simulations obtained for 100 different scenarios at SIL station (see Figure 10 for more explanations).

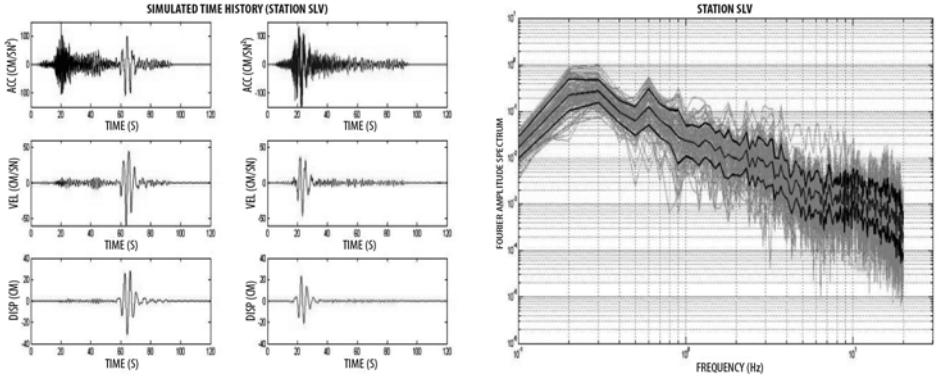

Figure 18. Broadband earthquake simulations obtained for 100 different scenarios at SLV station (see Figure 10 for more explanations).

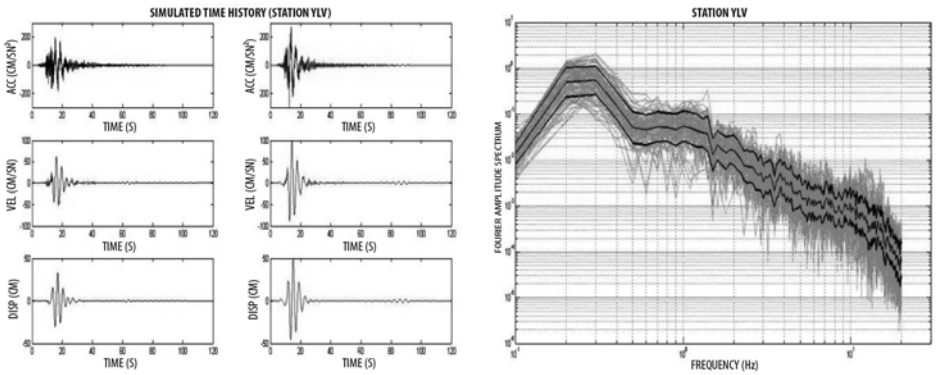

Figure 19. Broadband earthquake simulations obtained for 100 different scenarios at ARM station (see caption of Figure 10 for more explanations).

Acknowledgement

This study was financially supported by the research fund of Istanbul University Project No:1827 and by TÜBİTAK Project No: 108M584.

References

[1] Hutchings, L. And Wu, F., Empirical Green's Functions From Small Earthquakes: A Waveform Study of Locally Recorded Aftershocks of the San Fernando Earthquake, J. Geophys. Res., 95, 1187-1214, 1990.

[2] Fahjan, M. Y., Türkiye Deprem Yönetmeliği (DBYBHY,2007) Tasarım İvme Spektrumuna Uygun Gerçek Deprem Kayıtlarının Seçilmesi ve Ölçeklenmesi, İMO Teknik Dergi, 292, 4423-4444, 2008.

[3] Abrahamson, N. A., Non-stationary Spectral Matching Program RSPMATCH, PG&E Internal Report, 1998.

[4] Erdik, M., Durukal, E., Siyahi, B., Fahjan, Y., Şeşetyan, K., Demircioğlu, M., Akman, H., Depreme Dayanıklı Yapı Tasarımında Deprem Yer Hareketinin Belirlenmesi, Beşinci Ulusal Deprem Mühendisliği Konferansı, İstanbul, 26-30 Mayıs 2003.

[5] Bommer, J. J., Acevedo, A. B., Douglas, J., The Selection and Scaling of Real Earthquake Accelograms for Use in Seismic Design and Assesment, Proceedings of ACI International Conference on Seismic Bridge Design and Retrofit, American Concrete Institute, 2003.

[6] Naeim, F., Kelly, J. M., Design of Seismic Isolated Structures: From Theory to Practice, John Wiley &Sons, 1999.

[7] Barka, A.A., Slip distribution along the North Anatolian Fault associated with large earthquakes of the period 1939 to 1967, Bull. Seismol. Soc. Am., 86, 1238-1254.

[8] Toksoz, M.N., A.F. Shakal, and A.J. Micheal, Space-time migration of earthquakes along the North Anatolian Fault and seismic gaps, Pure Appl. Geophys, 117, 1258-1270.

[9] Pinar, A., Kuge, K., Honkuro, Y., Moment tensor inversion of recent small to moderate sized earthquakes: implications for seismic hazard and active tectonics beneath the Sea of Marmara. Geophys. J. Int., 153, 133–145, 2003.

[10] Hutchings, L., "Prediction" of Strong Ground Motion for the 1989 Loma Prieta Earthquake Using Empirical Green's Functions. Bull, Seismol. Soc. Am, 81, 88–121, 1991.

[11] Hadley, D. M., Helmberger D. V., Simulation of Strong Ground Motions. Bull. Seism. Soc. Am. , 70, 617-630, 1980.

[12] Boore, D. M., Stochastic Simulation of High-Frequency Ground Motions Based on Seismological Models of theRadiated Spectra, Bulletin of the Seismological Society of America 73, 1865-1894, 1983.

[13] Irikura, K., Semi-Empirical Estimation of Strong Ground Motions During Large Earthquakes. Bull. Disaster Prevention. Res. Inst Kyoto Univ. 33, 63–104, 1983.

[14] Kramer S. T., Geotechnical Earthquake Enginnering, Prentice-Hall, Inc, 1996.

[15] Hartzell, S. H., Earthquake Aftershocks as Green's Functions, Geophys.Res.Lett, 5, 1-4, 1978.

[16] Wu, F., Prediction of Strong Ground Motion Using Small Earthquakes, Proceedings of the 2nd International Conference on Microzonation. Vol II San Francisco, 701-704, 1978.

[17] Aki, K., Seismic Displacements Near a Fault, J. Geophys. Res., 73,5359-5376, 1968.

[18] Bouchon, M. Aki, K.., Discrete Wave-Number Representation of Seismic Wavefields, Bull. Seism.Soc. Am. 67, 259-277, 1977.

[19] Brune, J.N., Tectonic Stress and the Spectra of Seismic Shear Waves from Earthquakes, J. Geophys. Res.,75, 4997–5010, 1970, (Correction, J. Geophys. Res. 76 (20), 5002, 1971)

[20] McGuire R. K., Hanks, T.C., RMS Acceleration and Spectral Amplitudes of Strong Ground Motion During the San Fernando, California Earthquake, Bull. Seism.Soc. Am. 70, 1907-1919, 1980.

[21] Atkinson, G. M., Silva, W., Stochastic Modeling of California Ground Motions, , Bull. Seism.Soc. Am. 90, 255-274, 2000.

[22] Boore, D. M., Simulation of Ground Motion Using the Stochastic Method, Pure appl. Geophys. 160, 635-676, 2003.

[23] Beresnev, I., Atkinson, G., Modelling Finite Fault Radiation from the n Spectrum, Bull. Seism.Soc. Am. 87, 67-84,1997.

[24] Tanırcan, G., İstanbul için 3 boyutlu hız modeli ile yer hareketi simülasyonu, Gazi Üniversitesi Mühendislik Mimarlık Fakültesi Dergisi, Cilt 27, No 1, 27-35, 2012.

[25] Erdik M., Durukal, E., A Hybrid Procedure for the Assesment of Design Basis Earthquake Ground Motions for Near-Fault Conditions, Soil Dynamics and Earthquake Engineering, 21, 431-443, 2001.

[26] Pulido N, Ojeda A, Atakan K, Kubo T., Strong Ground Motion Estimation in the Sea of Marmara Region (Turkey) Based on a Scenario Earthquake, Tectonophysics, 391:357–374, 2004.

[27] Mathilde, B. S., Pulido, N., Atakan, K., Sensitivity of Ground Motion Simulations to Earthquake Source Parameters: A Case Study for Istanbul, Turkey, Bull. Seism.Soc. Am. 97, 881-900, 2007.

[28] Ansal, A., Akıncı, A., Cultera, G., Erdik, M., Pessina, V., Tönük, G., Ameri, G., Loss Estimataion in İstanbul Based on Deterministic Earthquake Scenarios of The Marmara Sea Region (Turkey), Soil Dynamics and Earthquake Engineering, 29, 699-709, 2009.

[29] Mert A., İstanbul İçin Tasarım Esaslı Kuvvetli Yer Hareketi Dalga Formlarının Zaman Ortamında Türetilmesi, Doktora Tezi, İstanbul Üniversitesi, Fen Bilimleri Enstitüsü, 2011.

[30] Okay, I.A., Demirbağ, E., Kurt, H., Okay, N., Kuşçu, İ., An active, Deep Marine Strike-Slip Basin Along the North Anatolian Fault in Turkey, Tectonics, V: 18, No: 1, 129-147, 1999.

[31] Okay, I.A., Kaşlılar Ö. A., İmren, C., Boztepe G. A., Demirbağ, E., Geometry of Active Faults and Strike Slip Basins in the Marmara Sea, Northwest Turkey: A Multichanel Seismic Reflection Study. NATO Advanced Research Seminar , May 14-17, 2000, Istanbul, Abstracts 20-21.

[32] İmren C., Le Pichon, X., Rangin C., Demirbağ E., Ecevitoğlu B., Görür N., The Anatolian fault within the Sea of Marmara: A new interpretation based on Multi channel seismic and multibeam bathymetry data, Earth Planet Sci Letter, 186, 143-158, 2001.

[33] Le Pichon, X., Sengör, A.M.C., Demirbag, E., Rangin, C., Imren, C., Armijo, R., Görür, N., Cagatay, N., Mercıer De Lepınay, B.,Meyer, B., Saatcılar, R., Tok, B., The active main Marmara fault. Earth Planet. Sci. Lett. 192, 595–616, 2001.

[34] Gökaşan, E., Alpar, B., Gazioğlu, C., Yücel, Z.Y., Tok, B., Doğan, E., Guneysu, C., Active Tectonics of the Izmit Gulf (NE Marmara Sea): from High Resolution Seismic and Multi-Beam Bathymetry Data, Mar Geol, 175(1–4):271–294, 2001.

[35] Armijo, R., Pondard, N., Meyer, B., Submarine Fault Scarps in the Sea of Marmara Pull-Apart North Anatolian Fault: Implications for Seismic Hazard in Istanbul, Geochem Geophys Geosyst, 6:Q06009:29., 2005.

[36] Pınar, A., Kuge, K., Honkura, Y., Moment Inversion of Recent Small to Moderate Sized Earthquakes: Implications for Seismic Hazard and Active Tectonics Beneath the Sea of Marmara, Geophys J Int, 153:133–145, 2003.

[37] Orgulu, G., Seismicity and Source Parameters for Small-Scale Earthquakes Along the Splays of the North Anatolian Fault (NAF) In the Marmara Sea, Geophysical Journal International 184, 385-404, 2011.

[38] Carton, H., Singh, S.C., Hirn, A., Bazin, S., Voogd, B., Vigner, A., Ricolleau, A., Cetin, S., Oçakoğlu, N., Karakoç., Sevilgen, V., Seismic imaging of the three-dimensional architecture of the Çınarcık Basin along North Anatolian Fault, Journal of Geophysical research, Vol. 112, 2007.

[39] Laigle, M., Becel, A., Voogd B., Hirn, A., Taymaz, T., Özalaybey, S., A first Deep Seismic Survey in the Sea of Marmara: Deep Basins and Whole Crust Architecture and Evoluation, Earth Planet. Sci. Lett. 270, 168-179, 2008.

[40] Becel, A., Laigle, M., Voogd, B., Hirn, A., Taymaz, T., Galve, A., Shimamura, H., Murai, Y., Lepine, J.C., Sapın, M., Özalaybey, S., Moho, Crustal Architecture and Deep Deformation Under the North Marmara Trough from the SEISMARMARA Leg 1 Offshore-Onshore Reflection-Refraction Survey, Tectonophysics, 467, 1-21, 2009.

[41] Yılmaz Y, Gökaşan E, Erbay AA., Morphotectonic Development of the Marmara Region. Tectonophysics doi:10.1016/j.tecto.2009.05.012, 2009.

[42] Oncel, A.O. & Wilson, T., Evaluation of earthquake potential along the Northern Anatolian Fault Zone in the Marmara Sea using comparisons of GPS strain and seismotectonics parameters. Tectonophysics., 418:205-218, 2006.

[43] Hanks T.C. & Kanamori H. A moment magnitude scale. J. Geophys. Res., 84, 2348-2350, 1979.

[44] Wells D.L. & Coppersmith K.J., New empirical relationships among magnitude, rupture length, rupture width, rupture area and surface displacement. Bull. Seism. Soc. Am., 84: 974-1002, 1994.

[45] Larsen S., E3D: 2D/3D Elastic Finite-Difference Wave Propagation Code, 1995.

[46] Karabulut H., Özalaybey S., Taymaz T., Aktar M., Selvi O., Kocaoğlu A., A Tomographic Image of the Shallow Crustal Structure in The Eastern Marmara, Geophys. Res. Lett., 30(24, 2777), 2003.

[47] Hutchings, L., Program NetMoment, a Simultaneous calculation of Moment, Source Corner Frequency, and Site Specific t* from Network Recordings, Lawrence Livermore National Laboratory, Livermore, CA, UCRL-ID 135693, 2001.

[48] Hutchings, L., Ioannidou, E., Kalogeras, I., Voulgaris, N., Savy, J., Foxall,W., Scognamiglio, L., Stavrakakis, G., A Physically-Based Strong Ground-Motion Prediction Methodology; Application to PSHA and the 1999 M=6.0 Athens Earthquake.Geophys. J. Int., 168,569–680, 2007.

[49] Akıncı, A., Malagnini, L., Herrmann, R. B., Gok, R., Sorensen, M. B., Ground Motion Scaling in the Marmara Region, Turkey, Geophys. J. Int. 166, 635-651, 2006.

[50] Lama, R.D. and Vutukuri, V.S., Handbook on Mechanical Properties of Rocks, Volume II: Testing Techniques and Results, Trans Tech. Publications, 1978, 245 pp., J. Phys. Earth. 42, 377–397, 1978.

[51] Prejean, S.G., Ellsworth, W.L., Observations of Earthquake Source Parameters and Attenuation at 2 km Depth in the Long Valley Caldera, Eastern California, Bull. Seismol. Soc. Am. ,91, 165–177, 2001.

[52] Scognamiglio L., Hutchings, L, A test of a Physically-based strong ground motion prediction methodology with the 26 September 1997, Mw=6.0 Colfiorito (Umbria-Marche Sequence), Italy earthquake, Tectonophysics, 476:145-158, 2009.

[53] Kostrov, B.V. and S. Das., Principles of earthquake source mechanics. In: Cambridge Monographs on Mechanics and Applied Mathematics, Cambridge University Press, Cambridge, 1988.

[54] Irikura, K. and K. Kamae:Estimation of strong ground motion in broad-frequency band based on a seismic source scaling model and an empirical Green's function technique, Annali Di Geofisica, Vol. XXXVII, N.6, 1721-1743, 1994.

[55] Beresnev, I. A. and G. M. Atkinson., Modeling finite-fault radiation from the wn spectrum, Bulletin of the Seismological Society of America 87: 67-84, 1997.

[56] Kamae, K., Irikura, K. ve Pitarka, A., "A Technique for Simulating Strong Ground motion using Hybrid Green's Function", Bull. Seism. Soc. Am., Cilt 88, No 2, 357-367, 1998.

[57] Hartzell, S., S. Harmsen, A. Frankel, and S. Larsen., Calculation of broadband time histories of ground motion: comparison of methods and validation using strong-ground motion from the 1994 Northridge earthquake, Bull. Seism. Soc. Am. 89: 1484–1504, 1999.

[58] Pitarka A., Somerville P., Fukushima Y., Uetake T., ve Irikura,K., "Simulation of Near-Fault Strong-Ground Motion Using Hybrid Green's Functions" Bull. Seism. Soc. Am. Cilt 90, 566-586, 2000.

[59] Pulido N., Ojeda, A., Kuvvet A. ve Kubo, T.,"Strong Ground Motion Estimation in the Sea Region (Turkey) Based on a Scenario Earthquake", Tectonophysics, Cilt 391, 357-374, 2004.

[60] Graves, R. W., and A. Pitarka., Broadband time history simulation using a hybrid approach, Proc. 13th World Conf. Earthq. Eng., Vancouver, Canada, paper no. 1098, 2004.

[61] Mena, B., E. Durukal, and M. Erdik. Effectiveness of hybrid Green'sfunction method in the simulation of near-field strong motion: An application to the 2004 Parkfield earthquake, Bull. Seismol. Soc.Am. 96, 183–205, 2006.

[62] Pulido, N., and M. Matsuoka. Broadband Strong Motion Simulation of the 2004 Niigata-ken Chuetsu Earthquake: Source and Site Effects. Third International Symposium on the Effects of Surface Geology on Seismic Motion, Grenoble, France, 1, 657-666, 2006.

[63] Liu, P., R. Archuleta, and S. H. Hartzell., Prediction of broadband ground motion time histories: Frequency method with correlation random source parameters, Bull. Seismol. Soc. Am. 96, 2118–2130, 2006.

[64] Rodgers, A. J., E. Matzel, M. Pasyanos, A. Petersson, B. Sjogreen, C. Bono, O. Vorobiev, T. Antoun, and W. Walter (2008). Seismic simulations using parallel computing and three dimensional Earth models to improve nuclear explosion phenomenology and monitoring, 30th Monitoring Research Review, Portsmouth, Virginia, 23–25 September 2008.

[65] Mai, P. M., J. Ripperger, J.-P. Ampuero, and J.-P. Hillers (2006). Frontiers in source modeling for near-source ground-motion prediction, in Proc. of the 3rd Int. Symp. on the Effects of Surface Geology on Seismic Motion, Grenoble, France, 30 August–1 September 97–114, 2006.

[66] Aki, K., Richards, P.G., Quan'itative Seismology, Theory and Methods, Volumes I and II, W. H. Freeman, New York, 1980.

[67] Abrahamson, N. A., and W. J. Silva., Summary of the Abrahamson and Silva NGA ground motion relations, Earthq. Spectra 24, no. S1,67–97, 2008.

[68] Boore, D. M., and G. M. Atkinson., Ground-motion prediction equations for the average horizontal component of PGA, PGV, and 5%-damped PSA at spectral periods between 0.01 s and 10.0 s, Earthquake Spectra 24, 99–113, 2008.

[69] Campbell, K. W., and Bozorgnia, Y., 2008. NGA ground motion model for the geometric mean horizontal component of PGA, PGV, PGD and 5% damped linear elastic response spectra for periods ranging from 0.01 to 10 s, Earthquake Spectra 24, 139-171, 2008.

[70] Erdik, M., Durukal, E., Şeşetyan, K., Istanbul için kuvvetli yer hareketi Benzeşimi ve yakın saha bölgelerindeki deprem hareketleri özelliklerinin belirlenmesi, Proje Raporu, Proje No:103I050, Istanbul, 2008.